How is spatial homogeneity in precipitation extremes changing globally?

Ankit Ghanghas[1], Ashish Sharma[2], Sayan Dey[1] and Venkatesh Merwade[1]

[1] Lyles School of Civil Engineering, Purdue University, West Lafayette, IN, USA

[2] School of Civil and Environmental Engineering, University of New South Wales, Sydney, New South Wales, Australia.

Corresponding author: Ankit Ghanghas (aghangha@purdue.edu)

Key Points:

- A global trend of moisture accumulation towards the storm center as spatial extent decreases with a rise in temperatures
- Rising temperature causes significant shrinking of precipitation extent in tropics, but an expansion in arid regions and central Europe.
- Storms with higher precipitation intensity show a faster decrease in spatial extent.

Abstract.

The effect of climate change on precipitation intensity is well documented. However, findings regarding changes in spatial extent of extreme precipitation events are still ambiguous as previous studies focused on particular regions and time domains. This study addresses this ambiguity by investigating the pattern of changes in the spatial extent of short duration extreme precipitation events globally. A grid-based indicator termed Spatial-Homogeneity (SH) is proposed and used to assess the changes of spatial extent in Global Precipitation Measurement (GPM) records. This study shows that i) rising temperature causes significant shrinking of precipitation extent in tropics, but an expansion of precipitation extent in arid regions, ii) storms with higher precipitation intensity show a faster decrease in spatial extent, iii) larger spatial extent storms are associated with higher total precipitable water. Results imply that in a warming climate, tropics may experience severe floods as storms may become more intense and spatially concentrated.

Plain Language Summary.

Variation in extreme precipitation patterns can significantly impact flood risk, ecology as well as the efficacy of water supply and management strategies. With a changing climate, there is an overarching need to understand how alterations in climate changes precipitation patterns, particularly those corresponding to extreme precipitation events. Analyzing the intensity (amount of rainfall/hour) of precipitation, spatial extent of the precipitation event, duration of the precipitation event and total volume of precipitated water are key to understanding these extreme precipitation events. There is a clear consensus among the scientific community that higher temperatures result in more intense precipitation events, but the effect of temperature on spatial extent is still debated. This study uses a new Spatial-Homogeneity metric to analyse the global changes in spatial extent of extreme precipitation storms. The study finds that a higher temperature results in smaller size extreme storms in the tropics, but larger size storms in the arid regions. It is also observed that more intense precipitation events have smaller spatial extent, implying that rising temperatures will result in spatially smaller and more intense extreme precipitation storms.

1 Introduction

The devastation from flash floods particularly in rapidly urbanizing environments is well documented, as intense precipitation storms can quickly turn into walls of water in highly impervious areas (Hapuarachchi et al., 2011). One of the greatest challenges to understanding flash floods is to understand the spatial and temporal distribution of precipitation, particularly of intense short period precipitation bursts (Archer & Fowler, 2018; Kelsch Matthew and Caporali, 2001). Knowledge of how such patterns change with time or with the intensity of the precipitation experienced, is of considerable use in designing effective stormwater systems and preparing for changes in climate.

The variation of extreme-precipitation intensity with temperature is well documented, underpinning the understanding of how extreme precipitation patterns might change in future (Hardwick Jones et al., 2010; Lenderink et al., 2011; Lenderink & van Meijgaard, 2008; Mishra et al., 2012; Utsumi et al., 2011; Westra et al., 2014). It is generally accepted that in a warming climate the intensity of an extreme precipitation will increase because precipitation depends on the atmospheric water content which increases exponentially with temperature, as governed by the Clausius-Clapeyron(C-C) relationship (Roderick et al., 2019, 2020; Trenberth et al., 2003; Visser et al., 2021).While global daily precipitation exhibits a sensitivity (or scaling) of around 6-7%/°C (C-C rate) with rise in temperature (Kharin et al., 2013; Pall et al., 2007; Tebaldi et al., 2006), short duration (sub-daily and sub-hourly) precipitation storms are observed to scale at rates ranging from C-C to 2 C-C (called super C-C scaling) (Berg et al., 2013; Hardwick Jones et al., 2010; Lenderink et al., 2017; Lenderink & van Meijgaard, 2008; Mishra et al., 2012; Westra et al., 2014). This super C-C scaling is hypothesized to be a result of change in storm dynamics, particularly the morphing of the storm extent and underlying structure (Collins et al., 2013; Lenderink & van Meijgaard, 2008).

Unlike the general acceptance of variation in intensity, the variation in the spatial extent of short duration storms is still debated with two contrasting hypotheses. The first hypothesis suggests a decreasing spatial extent with rising temperature due to dynamic factors dominating the storm dynamics, thereby redistributing the moisture towards the center (Figure 1a) (Wasko et al.,

2016). The second, contrasting, hypothesis, suggests that if the thermodynamic factors dominate, rising temperature would result in increasing spatial extent owing to stronger cloud dynamics and larger shower clusters which will bring more moisture from larger areas (Lochbihler et al., 2017). Findings from numerous studies analyzing the effect of temperature on spatial extent support the decreasing spatial extent hypothesis (Chang et al., 2016; Guinard et al., 2015; Han et al., 2020; J. Li et al., 2018; Peleg et al., 2018; Wasko et al., 2016), and several other support the increasing spatial extent hypothesis (Bevacqua et al., 2021; Chen et al., 2021; Lochbihler et al., 2017; Matte et al., 2022), while some others present no effect of temperature on spatial extent (Manola et al., 2018). However, most past studies have focused on specific regions, or on certain types of storms, or at daily precipitation extremes rather than short duration storms.

To address the ambiguity of whether short duration precipitation extents are expanding or shrinking with rising temperature, this study investigates the global patterns of change in spatial extent. This study proposes a novel metric to quantify grid-homogeneity termed Spatial-Homogeneity (SH) to compare the changes in spatial extent of extreme storms with different intensity and at different locations. The spatial-homogeneity metric can be used for radar as well as satellite measurements and is applicable for both short and long duration precipitation extremes. The study first investigates the global variability in spatial extent of short duration extreme storms in the recent past. Subsequently the relationship between temperature and spatial extent is examined. Finally, the study explores how total precipitable water, warm versus cold years and wet versus dry years impact the spatial extent.

Even though the satellite products are known to underestimate rainfall rates for deep convective systems (Adhikari et al., 2019; Dinku et al., 2010; Duan et al., 2015; Kucera & Klepp, 2022; R. Li et al., 2021), their high spatio-temporal resolution and global coverage make them useful in assessing change in the spatial extent of precipitation. Therefore, to have an acceptable global resolution, this study adopts satellite data products instead of the sparsely gauged ground observations available to represent variability in spatial extent across the world and to infer changes in this variability with local climatic variables including temperature, precipitation intensity and total precipitable water.

2 Data and Methods

The Integrated Multi-satellite Retrievals for Global Precipitation Measurement (IMERG) (version 6) dataset provides continuous records of satellite precipitation observation from 2000 - present, as the IMERG algorithm combines the early precipitation estimates from Tropical Rainfall Monitoring Mission (TRMM) (2000-2015) with the more recent precipitation estimates from Global Precipitation Measurement (GPM) (2014-present) (Huffman et al., 2020). However, to maintain the homogeneity of records only GPM IMERG estimates from 2014 to 2022 are used in this study. Due to the focus of this study on spatial extent of instantaneous/extreme precipitation bursts, analysis is performed on IMERG's high spatial and temporal resolution 3IMERGHH (version 6) (Huffman et al., 2020) product available at 0.1° X 0.1° spatial resolution and 30 minute time step. Earth ReAnalysis (ERA5), produced by European Center for Medium-Range Weather Forecasts (ECMWF), provides global reanalysis data for both temperature and moisture (Hersbach et al., 2020). ERA5 combines historical observations with the Integrated Forecasting System (IFS) Cy41r2 model to produce hourly outputs of numerous atmospheric, land and oceanic climate variables. Hourly Integrated Water Vapor (IWV) or Total Column Water Vapor (TCWV) at 0.25° X 0.25° spatial resolution is used in this study. Hourly 2m surface air temperature at 0.1° X 0.1° spatial resolution are obtained from the land component of ERA5, the ERA5-Land dataset (Muñoz-Sabater et al., 2021).

To analyze the spatial extent of extreme precipitation events, independent storm fields must be identified. In this study, a storm field is defined by considering a grid cell with extreme precipitation and its eight neighboring cells such that the center pixel corresponds to the center of the storm and receives more precipitation than the neighboring cells. To identify independent storm fields, the top ten Annual Maximum Precipitation (AMP) events at each grid cell of the GPM dataset are estimated for each year in the dataset. Further, for each grid cell, the precipitation for the eight neighboring cells surrounding the central precipitation event is extracted for the same time of occurrence as the central extreme precipitation event and compared to the center cell. If, for instance, the AMP event at the center cell has the same or lower precipitation than one of its eight neighbors, then the next maximum event (out of the top

ten annual maximum events) is considered and compared with neighboring precipitation at the time of its occurrence. The validity of independent storm field is enforced by choosing only the maximum event out of the top ten maximum events which has greatest intensity at the center cell than its neighbors.

A new metric, "Spatial Homogeneity" denoted SH, is proposed to investigate and compare the changes in spatial extent of varying intensity extreme storms and at different locations. To understand the homogeneity metric for an extreme storm, precipitation for all the cells in the storm field is sorted in descending order of its intensity and a cumulative normalization performed. Consider the precipitation in descending order is represented as $P_0, P_1, P_2, P_3, P_4, P_5, P_6, P_7, P_8$ where in P_0 is maximum precipitation and lies at the center of the storm field. The study ascertains the spatially accumulated precipitation average as $P_0/1, (P_0+P_1)/2, (P_0+P_1+P_2)/3, \ldots, (P_0+P_1+P_2+P_3+P_4+P_5+P_6+P_7+P_8)/9$. Here the last term represents average precipitation for the entire grid for the extreme storm event considered. These values are then plotted against the number of grid points considered in formulating the accumulated spatial average. The above accumulated precipitation distribution can be compared to the case where all neighbors have zero precipitation and only the center point received precipitation. In this scenario, the accumulated rainfall plot would represent $P_0/1, (P_0)/2, (P_0)/3 \ldots\ldots (P_0)/9$ against the number of grid points associated. The other comparison represented the case where all grid points receive the same amount of precipitation say P_0, resulting in a constant value (P_0) being depicted against the number of grid cells. An assessment of the spatial distribution of each storm is then formulated by noting how strongly the actual extreme event deviated from the two extreme cases considered. This assessment is depicted in Figure 1b giving an overview of the methodology adopted in assessing the spatial structure of the extreme precipitation event surrounding the central grid cell. The Spatial Homogeneity metric SH calculated using Equation 1 is used to ascertain the spatial homogeneity or inhomogeneity of the extreme storm field.

$$SH = \frac{a}{a+b} = \frac{\frac{1}{9} \times \sum_{i=0}^{8} P_i - \frac{P_0}{9}}{P_0 - \frac{P_0}{9}} \quad (1)$$

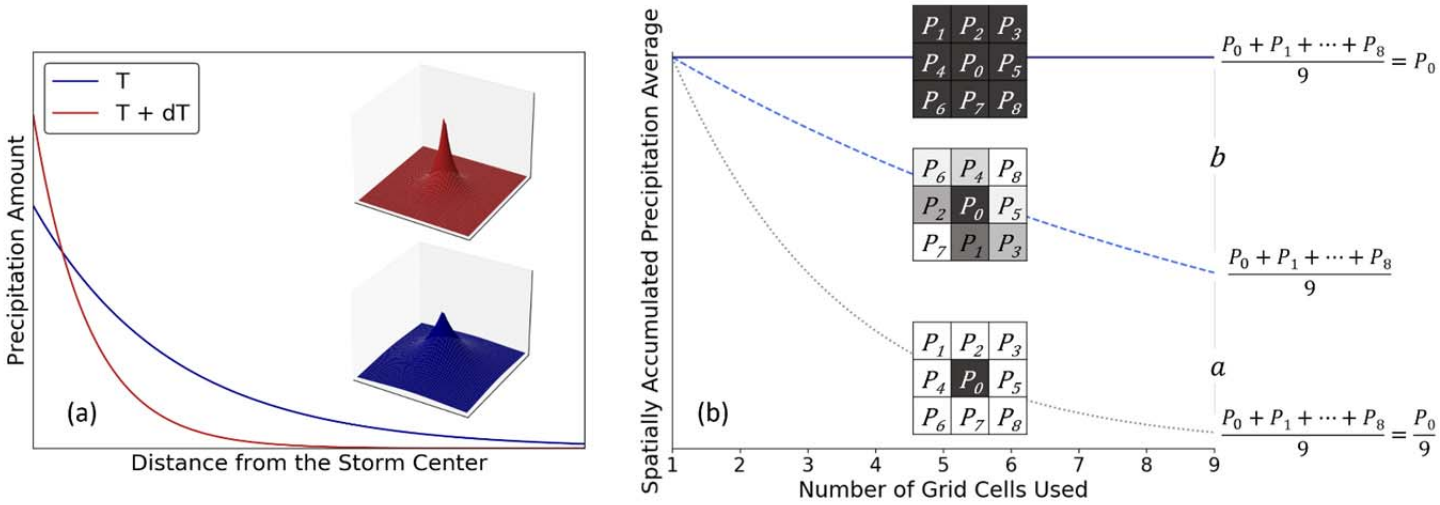

Figure 1. a) Depiction of increasing convection hypothesis, an increase in temperature results in higher intensity and redistribution of moisture towards storm center. Blue indicates lower temperature and red indicates higher temperature. Three-dimensional curves are also presented to emphasize the hypothesis. b) Representation of the SH methodology. Nine boxes represent the eight neighbors around the highest intensity center. The intensity of grey in each box indicates the intensity of rainfall at that grid.

166

167 The Spatial Homogeneity metric allows a comparison of the extreme storm from a fully uniform
168 case to a case where an isolated extreme falls at the center of the grid. If a warmer future creates
169 more isolated and convective rainfall events, the above metric will collapse to zero. If the
170 opposite were to occur (more uniform rainfall extremes) the metric will assume a value of one.
171 The increasing convection hypothesis outlined above is depicted in Figure 1a. The SH metric
172 allows assessment of spatial distribution of extreme precipitation events without focusing on the
173 intensity of the event as well as assessment of the spatial distribution of extreme events across
174 the world.

175 A sensitivity assessment of SH with associated temperature is performed using quantile
176 regression with a focus on the median (50th percentile). The resulting regression coefficient is
177 referred to as "sensitivity" in the remainder of this paper. The quantile regression sensitivity
178 estimator by Wasko & Sharma (2014) has been adopted in this study. As only annual maximum
179 precipitation (AMP) events are considered, the assessment results presented focus on the 50th
180 percentile (median) instead of rarer percentiles. Details of the sensitivity estimation procedure,

its sensitivity to computational needs, and its motivation in the context of identifying trends in a highly variable response, are presented in Wasko & Sharma (2014) and Sharma et al. (2018).

3 Results

3.1.Changes in of Spatial Homogeneity (Spatial Extent) in recent past

The Spatial-Homogeneity metric does not give a quantitative estimate of the exact spatial extent of the storm, but it is a quick and resourceful method to track the changes in spatial extent of storm. The SH-metric can also be used to understand the geographic distribution of spatial extent across the globe. The average SH-metric for AMP 30-min storms (Figure S1 in supporting information) shows smaller storm extents in tropics and mountainous regions. This is coherent with the findings of Tan et al. (2021), which concluded that extreme storms in tropics are typically smaller than those in northern and southern temperate regions.

Figure 2 presents the average change in SH between 2014 to 2021 with reference to the 2014 SH. A running median of 4°X4° grid has been used to smooth out the variability. The changes in SH from year to year are presented in Figure S2 in supporting information. The spatial extent of storms in the equatorial regions between 20° N and 20° S has increased homogenously over the years. The equator observes a significant and spatially consistent increase in spatial extent of storms. On the other hand, regions north of 30° N and south of 30° S have experienced spatially smaller storms in the recent years. The change of storm extent in these regions are inconsistent and sporadic increase in storm size can also be observed. Storms in the Arabian Peninsula, some parts of Africa near Mozambique and Madagascar, Mexico and parts of South America near Peru and Bolivia have consistently and significantly increased over the recent years. Contrasting results are observed in Northwest Africa around Morocco and Western Sahara, southern Argentina (Patagonian Dessert), and southern Australia, where storm sizes have consistently and significantly decreased in the immediate past.

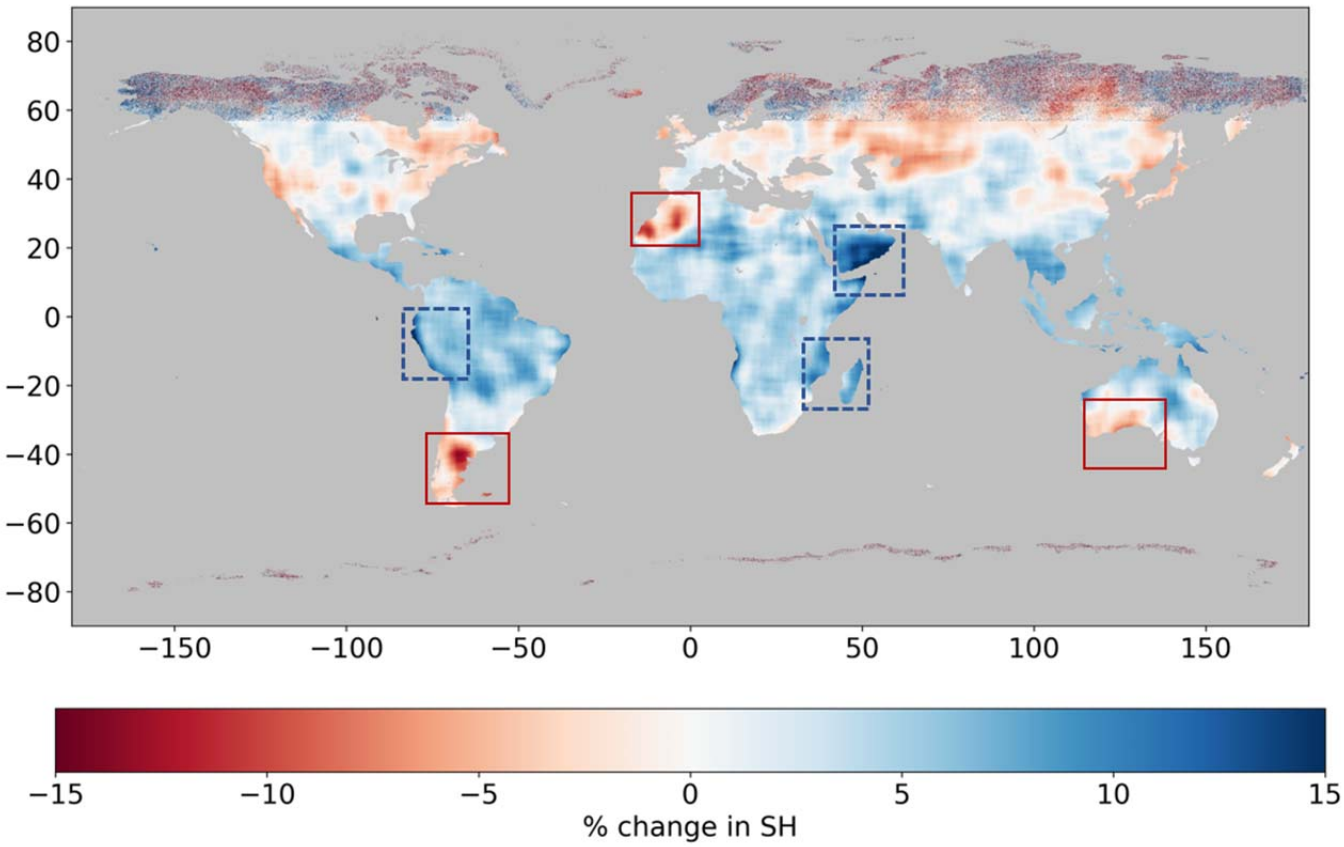

Figure 2. A 4°X4° median of Average Change in SH between 2014 to 2021 with reference to 2014 SH. Decrease in SH (spatial extent) is shown in red and increase in SH (spatial extent) is shown in blue. Boxes highlight regions with significant SH change, red box highlight decrease and blue-dashed box highlight increase.

3.2. Sensitivity of Spatial Homogeneity (Spatial Extent) to temperature.

To comprehensively understand the effect of local climate and atmosphere on the spatial extent of extreme storms, a sensitivity analysis of spatial extent with temperature, intensity of precipitation and total column water vapor is performed. Sensitivity of spatial extent with instantaneous temperature is presented in Figure 3. A 1°X1° moving median is applied to smooth out the variability. ERA5-land provides hourly temperature data, but GPM provides 30-min precipitation so the instantaneous temperature here refers to the temperature at the time of the storm or in the hour before the storm. It is evident from the study that the tropical regions

dominated by convective precipitation have strong negative relation between spatial extent and instantaneous temperature. This implies that as temperature rises, the convective storms in tropics shrink in size and the moisture concentrates at the center. Parts of the Amazon and Indonesian Tropical Regions observe 4-5%/°C reduction in spatial extent. On the other hand, the arid regions particularly Eastern Sahara, the Thar desert in India, Southern Arabian Peninsula, Gobi Desert and Western Coast of United States show positive sensitivity and will observe spatially larger storms with the warming climate. The northern and southern temperate regions generally present slight positive sensitivity of spatial extent with temperature with slightly negative sensitivity seen in central and northern Europe (0.1-1%/°C), southern New Zealand and Southern Argentina (Patagonian Dessert) (0.1-1.5%/°C).

This study uses instantaneous temperature rather than widely used mean daily temperature (Lenderink & van Meijgaard, 2008) because in case of convective storms, particularly in the tropics, temperature tends to drop at the advent of the storm and using daily temperature for sensitivity will result in inaccurate conclusions (Ali et al., 2018; Ali & Mishra, 2017). On comparing the results of Figure S3 and Figure 3, it is evident that the impact of using daily versus instantaneous temperature is concentrated in the equatorial regions. (Figure S3 in supporting information presents the sensitivity of spatial extent with mean daily temperature). Moreover, the sensitivity of spatial extent with instantaneous temperature is consistent and is conformable to the recommendations by (Visser et al., 2020).

The results from this study are coherent with the findings from both Wasko et al. (2016) and Lochbihler et al. (2017) which published contrasting results. While Wasko et al. (2016) concluded a reduction in spatial extents in Australia, Lochbihler et al. (2017) concluded an increase in spatial extent in Netherlands. This study finds that both the findings are accurate and the behavior of spatial extent with temperature is indeed dependent on the geographic location and the local climate.

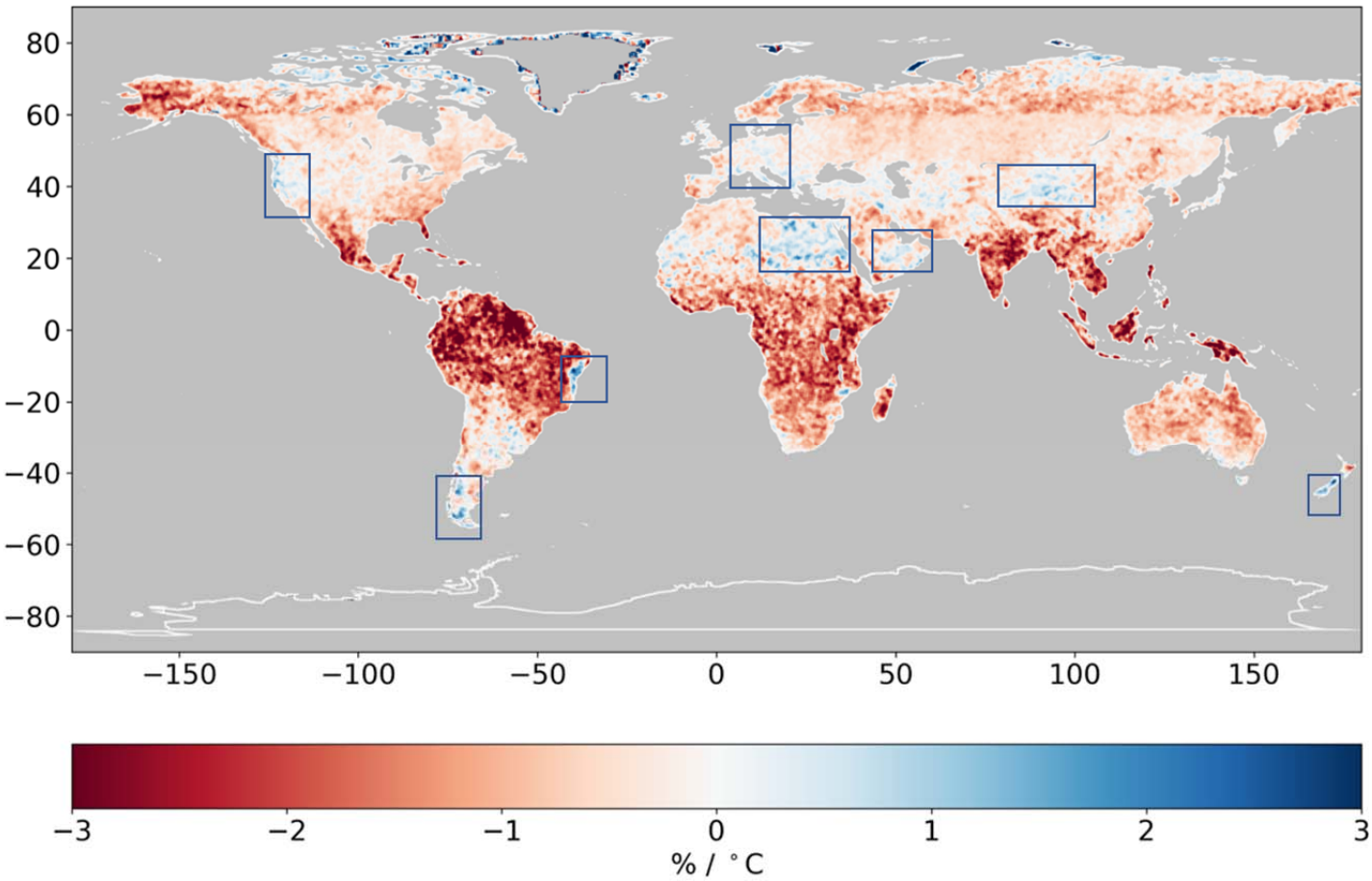

Figure 3. 1°X1° median of 50th percentile quantile regression of SH with instantaneous temperature. Negative sensitivity (decrease in SH with rising temperatures) is shown in red and Positive sensitivity (increase in SH with rising temperature) is shown in blue. Blue boxes highlight regions with negative sensitivity.

3.3. Effect of local climate on Spatial Homogeneity (Spatial Extent).

To assess the impact of local climate on SH, variation of the difference in SH associated with: maximum and minimum intensity storm (Figure 4a), maximum total column water vapor and minimum total column water vapor (Figure 4b), wettest and driest year storm (Figure 4c), and warmest and coldest year storm (Figure 4d) is mapped. At any location, the annual maxima storm with maximum precipitation intensity / maximum accumulated total column water vapor in 24hr prior to the storm is compared to the annual storm with minimum precipitation intensity / minimum accumulated total column water vapor in 24hr prior to the storm. Among the 2014-2021 period, the wettest and driest years at any location are estimated by comparing the total

annual precipitation, and warmest and coldest year are estimated by comparing the mean annual temperature.

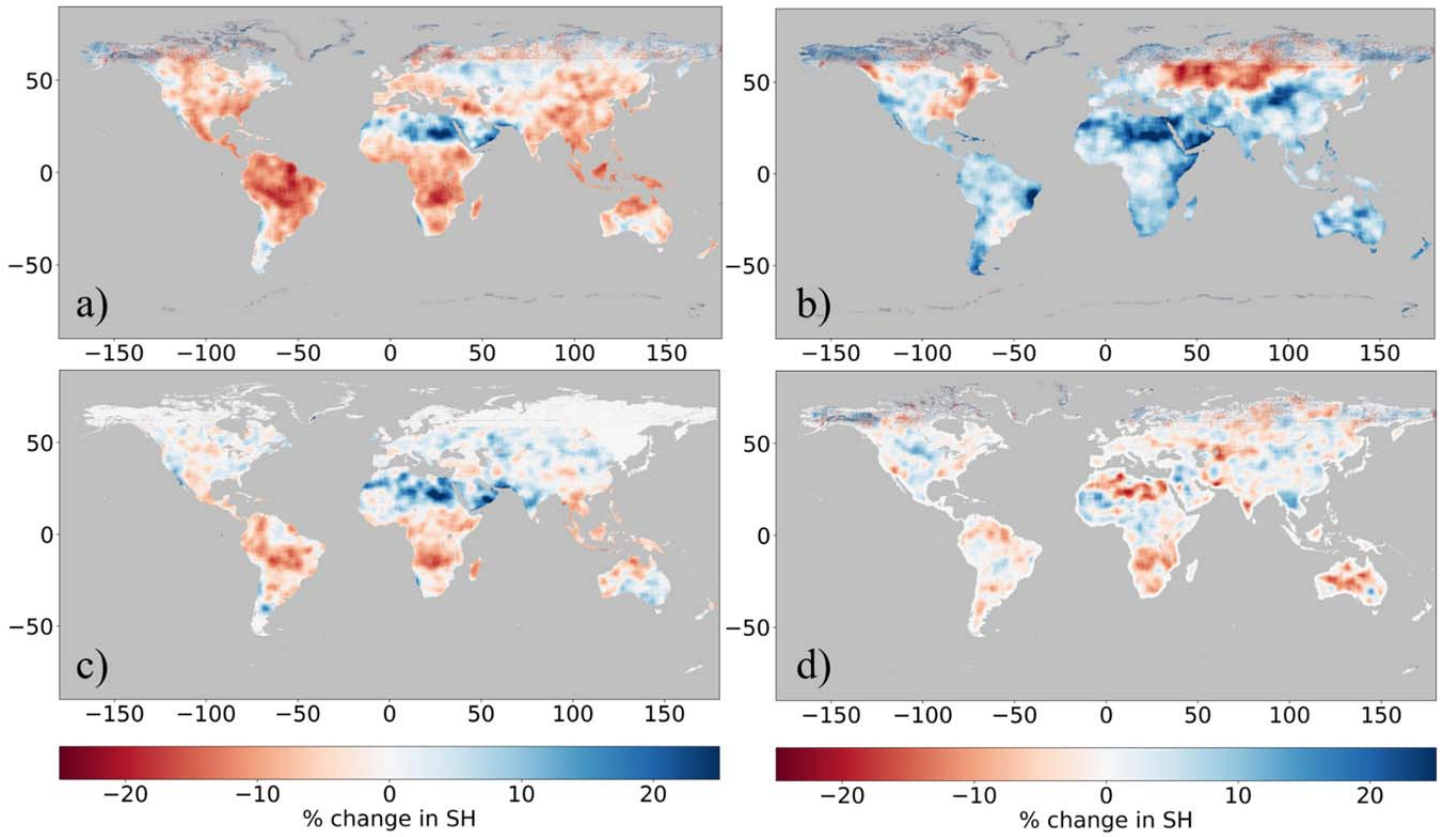

Figure 4. Change in SH when comparing SH corresponding to (a) Maximum vs Minimum Intensity storms, (b) Maximum vs Minimum Total Column Water Vapor Storms, (c) Wettest vs Driest Year storms and (d) Warmest vs Coldest Storms. Red indicates decrease in SH and blue indicates increase in SH

The overall trend indicates that globally a rise in intensity of storms leads to a lower spatial extent (Figure 4a). A larger spatial extent for more intense storms is observed in Sahara, Arabian Peninsula, Central Russia, and southern Argentina (Patagonian Dessert). The overall global trend corroborates with the findings by Wasko et al. (2016) for Australia (extended here to a global scale) that the moisture is being redistributed from storm boundaries to the storm center. The findings from Figure 4a and Figure 3 support the hypothesis presented in Figure 1a implying that a rise in temperature will result in more intense and spatially concentrated extreme storm bursts. Moreover, the findings by Lochbihler et al. (2017) are also corroborated in Arid Regions around

277 the world. On the other hand, total column water vapor (TCWV) has an overall reinforcing
278 relation with the SH. A rise in TCWV results in greater SH implying that at most locations, with
279 exceptions of Eastern US and around central Russia, spatially larger storms are associated with
280 higher TCWV (Figure 4b). The effect of total annual precipitation is regionally distinct as
281 Sahara, Arabian Peninsula, India, Central Asia and Europe have larger spatial extent storms in
282 wetter years. On the other hand, drier years observe larger spatial extent storms in tropical
283 regions in Southern America, Africa, South East Asia and Northern and Western Australia.
284 (Figure 4c). Mean annual temperature does not have a overall strong impact on SH globally and
285 difference in SH is evenly distributed with least variance among all the variables (Figure 4d).
286 The study here presents a preliminary analysis of the impact of local climate variables on change
287 in spatial extent and a more extensive analysis may result in significant regional trends.
288
289 **4. Discussion**
290
291 While the data length used in the study is shorter than that used for point-based studies of spatial
292 extent done in the past, it is interesting to note that the same conclusions are drawn from short
293 time period as the conclusions from longer duration time period (Figure S4 in supplementary
294 information provides sensitivity of SH with temperature for a time period of 2005-2021).
295
296 The study uses 9 grid cells (3x3 grid) to define the storm field and estimate SH. This 9-cell grid
297 structure implies that the storm field extends over 30x30 km which will be smaller than that
298 observed for daily storms, but it is sufficient for short duration (30 min) precipitation extremes. It
299 is noteworthy that using a larger size storm field (25 neighboring grid cells or more)
300 quantitatively changes the overall SH for short duration storms (Figure S5 (b)) however, using a
301 larger storm field does not alter the patterns for change in SH. The overall conclusions regarding
302 sensitivity of spatial extent (SH) with temperature and other parameters remain the same whether
303 using 9-cell storm field or 25-cell storm field (Figure S6).
304
305 These short duration storm systems are susceptible to presence of zero precipitation cells in the
306 storm field thus presenting larger inhomogeneity and less linearity in spatially accumulated
307 average precipitation. Although, the formulation of SH metric uses linear proportionality to

estimate the spatial homogeneity, a sensitivity analysis using non-linear proportionality to calculate SH does not significantly alter SH estimates. This establishes that linear proportionality can capture the spatial homogeneity even for short duration storms. It is also noteworthy that the zero-precipitation cells primarily affect SH for precipitation sparse arid regions (Figure S5(a)) which are hotspots for increasing spatial extent with temperature.

5. Conclusions

There is clear understanding that intensity of extreme storms will increase with increase in temperature but the studies on the spatial organization of storms have been conflicting. Use of daily average temperatures instead of sub-daily temperatures, focus on specific regions, or on certain type of storms, or at daily precipitation extremes rather than short duration storms; contributed to conflicting results in previous studies. The results of this study show that the geographic location and the local climate play a crucial role in how moisture is being distributed around a storm, particularly for short duration extreme storms. The following conclusions are drawn from this study:

1. Spatial extent of short duration precipitation extremes has increased in the equatorial tropics and decreased in the northern and southern temperate in the recent past. However, sensitivity of spatial extent with temperature has contrasting results.
2. An overall global trend of moisture accumulation towards the storm center as spatial extent decreases with a rise in temperatures.
3. Spatial extent of storms in arid regions (excluding Australia) and parts of central Europe tends to increase with increasing temperature.

Some other conclusions from the preliminary analysis with local climate variables can also be made. Higher intensity storms typically result in lower spatial extent storms. Furthermore, the study finds that spatially larger storms are globally associated with higher total precipitable water. Wet years in Sahara, Arabian Peninsula, India, Central Asia and Europe have larger spatial extent storms whereas dry years observe larger spatial extent storms in tropical regions in Southern America, Africa, Southeast Asia, Northern and Western Australia. Warm vs Cold year

do not have a consistent impact on spatial extent, although a more regressive analysis will result in concrete conclusions.

These results along with previous understanding that intensity of extreme storms increase in warmer climate, have significant implications as short duration extreme storms in warmer climate will be more intense and concentrated. If these trends of spatial extent continue as the global temperature rise, the tropics may experience intense and concentrated storms which may lead to severe floods.

Future studies may focus on analyzing if similar patterns on change in spatial extent (spatial homogeneity) are observed for longer duration storms. This study concludes that short (sub-hourly) extreme storms show significant change alteration in spatial extent, however the change in spatial extent may not be equally conspicuous for longer duration storms. This is routed in the fact that super CC scaling is observed for shorter (sub-hourly, hourly, sub-daily) duration storms and becomes less prominent as the duration of storm increases.

Data Availability Statement

All observational datasets and model simulations used in this study are publicly available. ERA5 and ERA5-Land are available from the European Centre for Medium-Range Weather Forecasts' (ECMWF) Copernicus Climate Change Service (C3S) Climate Date Store at https://cds.climate.copernicus.eu/cdsapp#!/dataset/reanalysis-era5-land?tab=overview and https://cds.climate.copernicus.eu/cdsapp#!/dataset/reanalysis-era5-pressure-levels?tab=overview. GPM IMERG data are available at https://gpm.nasa.gov/data.

References

Adhikari, A., Liu, C., & Hayden, L. (2019). Uncertainties of GPM Microwave Imager Precipitation Estimates Related to Precipitation System Size and Intensity. *Journal of Hydrometeorology*, *20*(9), 1907–1923. https://doi.org/10.1175/JHM-D-19-0038.1

Ali, H., Fowler, H. J., & Mishra, V. (2018). Global Observational Evidence of Strong Linkage Between Dew Point Temperature and Precipitation Extremes. *Geophysical Research Letters*, *45*(22), 12, 312–320, 330. https://doi.org/10.1029/2018GL080557

Ali, H., & Mishra, V. (2017). Contrasting response of rainfall extremes to increase in surface air and dewpoint temperatures at urban locations in India. *Scientific Reports*, *7*(1), 1228. https://doi.org/10.1038/s41598-017-01306-1

Archer, D. R., & Fowler, H. J. (2018). Characterising flash flood response to intense rainfall and impacts using historical information and gauged data in Britain. *Journal of Flood Risk Management*, *11*(S1), S121–S133 https://doi.org/10.1111/jfr3.12187

Berg, P., Moseley, C., & Haerter, J. O. (2013). Strong increase in convective precipitation in response to higher temperatures. *Nature Geoscience*, *6*(3), 181–185. https://doi.org/10.1038/ngeo1731

Bevacqua, E., Shepherd, T. G., Watson, P. A. G., Sparrow, S., Wallom, D., & Mitchell, D. (2021). Larger Spatial Footprint of Wintertime Total Precipitation Extremes in a Warmer Climate. *Geophysical Research Letters*, *48*(8), e2020GL091990. https://doi.org/10.1029/2020GL091990

Chang, W., Stein, M. L., Wang, J., Kotamarthi, V. R., & Moyer, E. J. (2016). Changes in Spatiotemporal Precipitation Patterns in Changing Climate Conditions. *Journal of Climate*, *29*(23), 8355–8376. https://doi.org/10.1175/JCLI-D-15-0844.1

Chen, Y., Paschalis, A., Kendon, E., Kim, D., & Onof, C. (2021). Changing Spatial Structure of Summer Heavy Rainfall, Using Convection-Permitting Ensemble. *Geophysical Research Letters*, *48*(3), e2020GL090903. https://doi.org/10.1029/2020GL090903

Collins, M., Knutti, R., Arblaster, J., Dufresne, J., Fichefet, T., Friedlingstein, P., Gao, X., Gutowski, W., Johns, T., Krinner, G., Shongwe, M., Tebaldi, C., Weaver, A., & Wehner, M. (2013). Long-term Climate Change: Projections, Commitments and Irreversibility. In: Climate Change 2013: The Physical Science. *Climate Change 2013 the Physical Science Basis: Working Group I Contribution to the Fifth Assessment Report of the Intergovernmental Panel on Climate Change*, *January 2014*.

Dinku, T., Connor, S. J., & Ceccato, P. (2010). Comparison of CMORPH and TRMM-3B42 over mountainous regions of Africa and South America. *Satellite Rainfall Applications for*

Surface Hydrology, 193–204. https://doi.org/10.1007/978-90-481-2915-7_11/FIGURES/11_5_164676_1_EN

Duan, Y., Wilson, A. M., & Barros, A. P. (2015). Scoping a field experiment: Error diagnostics of TRMM precipitation radar estimates in complex terrain as a basis for IPHEx2014. *Hydrology and Earth System Sciences*, *19*(3), 1501–1520. https://doi.org/10.5194/HESS-19-1501-2015

Guinard, K., Mailhot, A., & Caya, D. (2015). Projected changes in characteristics of precipitation spatial structures over North America. *International Journal of Climatology*, *35*(4), 596–612. https://doi.org/10.1002/joc.4006

Han, X., Mehrotra, R., & Sharma, A. (2020). Measuring the spatial connectivity of extreme rainfall. *Journal of Hydrology*, *590*, 125510. https://doi.org/10.1016/j.jhydrol.2020.125510

Hapuarachchi, H. A. P., Wang, Q. J., & Pagano, T. C. (2011). A review of advances in flash flood forecasting. *Hydrological Processes*, *25*(18), 2771–2784. https://doi.org/10.1002/hyp.8040

Hardwick Jones, R., Westra, S., & Sharma, A. (2010). Observed relationships between extreme sub-daily precipitation, surface temperature, and relative humidity. *Geophysical Research Letters*, *37*(22). https://doi.org/10.1029/2010GL045081

Hersbach, H., Bell, B., Berrisford, P., Hirahara, S., Horányi, A., Muñoz-Sabater, J., Nicolas, J., Peubey, C., Radu, R., Schepers, D., Simmons, A., Soci, C., Abdalla, S., Abellan, X., Balsamo, G., Bechtold, P., Biavati, G., Bidlot, J., Bonavita, M., … Thépaut, J.-N. (2020). The ERA5 global reanalysis. *Q J R Meteorol Soc*, *146*, 1999–2049. https://doi.org/10.1002/qj.3803

Huffman, G. J., Bolvin, D. T., Braithwaite, D., Hsu, K.-L., Joyce, R. J., Kidd, C., Nelkin, E. J., Sorooshian, S., Stocker, E. F., Tan, J., Wolff, D. B., & Xie, P. (2020). Integrated Multi-satellite Retrievals for the Global Precipitation Measurement (GPM) Mission (IMERG). In V. Levizzani, C. Kidd, D. B. Kirschbaum, C. D. Kummerow, K. Nakamura, & F. J. Turk (Eds.), *Satellite Precipitation Measurement: Volume 1* (pp. 343–353). Springer International Publishing. https://doi.org/10.1007/978-3-030-24568-9_19

Kelsch Matthew and Caporali, E. and L. L. G. (2001). Hydrometeorology of Flash Floods. In J. Gruntfest Eve and Handmer (Ed.), *Coping With Flash Floods* (pp. 19–35). Springer Netherlands. https://doi.org/10.1007/978-94-010-0918-8_4

Kharin, V. v, Zwiers, F. W., Zhang, X., & Wehner, M. (2013). Changes in temperature and precipitation extremes in the CMIP5 ensemble. *Climatic Change*, *119*(2), 345–357. https://doi.org/10.1007/s10584-013-0705-8

Kucera, P. A., & Klepp, C. (2022). Evaluation of high-resolution satellite precipitation over the global oceans. *Precipitation Science*, 305–332. https://doi.org/10.1016/B978-0-12-822973-6.00008-1

Lenderink, G., Barbero, R., Loriaux, J. M., & Fowler, H. J. (2017). Super-Clausius–Clapeyron Scaling of Extreme Hourly Convective Precipitation and Its Relation to Large-Scale Atmospheric Conditions. *Journal of Climate*, *30*(15), 6037–6052. https://doi.org/10.1175/JCLI-D-16-0808.1

Lenderink, G., Mok, H. Y., Lee, T. C., & van Oldenborgh, G. J. (2011). Scaling and trends of hourly precipitation extremes in two different climate zones – Hong Kong and the Netherlands. *Hydrology and Earth System Sciences*, *15*(9), 3033–3041. https://doi.org/10.5194/hess-15-3033-2011

Lenderink, G., & van Meijgaard, E. (2008). Increase in hourly precipitation extremes beyond expectations from temperature changes. *Nature Geoscience*, *1*(8), 511–514. https://doi.org/10.1038/ngeo262

Li, J., Wasko, C., Johnson, F., Evans, J. P., & Sharma, A. (2018). Can Regional Climate Modeling Capture the Observed Changes in Spatial Organization of Extreme Storms at Higher Temperatures? *Geophysical Research Letters*, *45*(9), 4475–4484. https://doi.org/10.1029/2018GL077716

Li, R., Wang, K., & Qi, D. (2021). Event-Based Evaluation of the GPM Multisatellite Merged Precipitation Product From 2014 to 2018 Over China: Methods and Results. *Journal of Geophysical Research: Atmospheres*, *126*(1), e2020JD033692. https://doi.org/10.1029/2020JD033692

Lochbihler, K., Lenderink, G., & Siebesma, A. P. (2017). The spatial extent of rainfall events and its relation to precipitation scaling. *Geophysical Research Letters*, *44*(16), 8629–8636. https://doi.org/10.1002/2017GL074857

Manola, I., van den Hurk, B., de Moel, H., & Aerts, J. C. J. H. (2018). Future extreme precipitation intensities based on a historic event. *Hydrology and Earth System Sciences*, *22*(7), 3777–3788. https://doi.org/10.5194/hess-22-3777-2018

Matte, D., Christensen, J. H., & Ozturk, T. (2022). Spatial extent of precipitation events: when big is getting bigger. *Climate Dynamics*, *58*(5), 1861–1875. https://doi.org/10.1007/s00382-021-05998-0

Mishra, V., Wallace, J. M., & Lettenmaier, D. P. (2012). Relationship between hourly extreme precipitation and local air temperature in the United States. *Geophysical Research Letters*, *39*(16). https://doi.org/10.1029/2012GL052790

Muñoz-Sabater, J., Dutra, E., Agust-Panareda, A., Albergel, C., Arduini, G., Balsamo, G., Boussetta, S., Choulga, M., Harrigan, S., Hersbach, H., Martens, B., Miralles, D. G., Piles, M., Rodr\'{\i}guez-Fernández, N. J., Zsoter, E., Buontempo, C., & Thépaut, J.-N. (2021). ERA5-Land: a state-of-the-art global reanalysis dataset for land applications. *Earth System Science Data*, *13*(9), 4349–4383. https://doi.org/10.5194/essd-13-4349-2021

Pall, P., Allen, M. R., & Stone, D. A. (2007). Testing the Clausius–Clapeyron constraint on changes in extreme precipitation under CO2 warming. *Climate Dynamics*, *28*(4), 351–363. https://doi.org/10.1007/s00382-006-0180-2

Peleg, N., Marra, F., Fatichi, S., Molnar, P., Morin, E., Sharma, A., & Burlando, P. (2018). Intensification of Convective Rain Cells at Warmer Temperatures Observed from High-Resolution Weather Radar Data. *Journal of Hydrometeorology*, *19*(4), 715–726. https://doi.org/10.1175/JHM-D-17-0158.1

Roderick, T. P., Wasko, C., & Sharma, A. (2019). Atmospheric Moisture Measurements Explain Increases in Tropical Rainfall Extremes. *Geophysical Research Letters*, *46*(3), 1375–1382. https://doi.org/10.1029/2018GL080833

Roderick, T. P., Wasko, C., & Sharma, A. (2020). An Improved Covariate for Projecting Future Rainfall Extremes? *Water Resources Research*, *56*(8), e2019WR026924. https://doi.org/10.1029/2019WR026924

Sharma, A., Wasko, C., & Lettenmaier, D. P. (2018). If Precipitation Extremes Are Increasing, Why Aren't Floods? *Water Resources Research*, *54*(11), 8545–8551. https://doi.org/10.1029/2018WR023749

Tan, X., Wu, X., & Liu, B. (2021). Global changes in the spatial extents of precipitation extremes. *Environmental Research Letters*, *16*(5), 54017. https://doi.org/10.1088/1748-9326/abf462

Tebaldi, C., Hayhoe, K., Arblaster, J. M., & Meehl, G. A. (2006). Going to the Extremes. *Climatic Change*, *79*(3), 185–211. https://doi.org/10.1007/s10584-006-9051-4

Trenberth, K. E., Dai, A., Rasmussen, R. M., & Parsons, D. B. (2003). THE CHANGING CHARACTER OF PRECIPITATION. *Bulletin of the American Meteorological Society*, *84*(9), 1205–1217. http://www.jstor.org/stable/26216879

Utsumi, N., Seto, S., Kanae, S., Maeda, E. E., & Oki, T. (2011). Does higher surface temperature intensify extreme precipitation? *Geophysical Research Letters*, *38*(16). https://doi.org/10.1029/2011GL048426

Visser, J. B., Wasko, C., Sharma, A., & Nathan, R. (2020). Resolving Inconsistencies in Extreme Precipitation-Temperature Sensitivities. *Geophysical Research Letters*, *47*(18), e2020GL089723. https://doi.org/10.1029/2020GL089723

Visser, J. B., Wasko, C., Sharma, A., & Nathan, R. (2021). Eliminating the "Hook" in Precipitation–Temperature Scaling. *Journal of Climate*, *34*(23), 9535–9549. https://doi.org/10.1175/JCLI-D-21-0292.1

Wasko, C., & Sharma, A. (2014). Quantile regression for investigating scaling of extreme precipitation with temperature. *Water Resources Research*, *50*(4), 3608–3614. https://doi.org/10.1002/2013WR015194

Wasko, C., Sharma, A., & Westra, S. (2016). Reduced spatial extent of extreme storms at higher temperatures. *Geophysical Research Letters*, *43*(8), 4026–4032. https://doi.org/10.1002/2016GL068509

Westra, S., Fowler, H. J., Evans, J. P., Alexander, L. v, Berg, P., Johnson, F., Kendon, E. J., Lenderink, G., & Roberts, N. M. (2014). Future changes to the intensity and frequency of short-duration extreme rainfall. *Reviews of Geophysics*, *52*(3), 522–555. https://doi.org/10.1002/2014RG000464